치의과학박사학위논문

The effect of additional segmental osteotomies of jaw on the changes of the pharyngeal airway space in the orthognathic surgery for mandibular setback movement

하악 후방이동 악교정수술에서 부가적인 악골의 분절골절단술이 상기도 공간 변화에 미치는 영향에 대한 연구

2020년 2월

서울대학교 대학원

치의과학과 구강악안면외과학전공

조 예 원

The effect of additional segmental osteotomies of jaw on the changes of the pharyngeal airway space in the orthognathic surgery for mandibular setback movement

지도교수 김 성 민

이 논문을 치의과학박사 학위논문으로 제출함

2019년 11월

서울대학교 대학원

치의과학과 구강악안면외과학전공

조 예 원

조예원의 박사 학위논문을 인준함

2019 년 12월

위 원 장　서 병 무　(인)

부위원장　김 성 민　(인)

위　　원　최 진 영　(인)

위　　원　김 태 우　(인)

위　　원　황 순 정　(인)

Abstract

The effect of additional segmental osteotomies of jaw on the changes of the pharyngeal airway space in the orthognathic surgery for mandibular setback movement.

Yewon Joh, D.D.S..

Program in Oral and Maxillofacial Surgery,

Department of Dental Science,

Graduate School, Seoul National University

Background and purpose: Patients who underwent orthognathic surgery that included a large amount of mandibular setback (SB) may suffer from sleep apnea or snoring due to airway space reduction. To increase airway space, palatal expansion and maxillary ASO can be combined. And to reduce the amount of mandibular SB movement, bilateral sagittal split ramus osteotomy (BSSRO) combined with anterior segmental osteotomy (ASO) can be applied. This study aimed to evaluate the effect of BSSRO combined with other osteotomies on the reduction of mandibular SB and the corresponding perioperative change on volume of the pharyngeal airway space (PAS).

Materials and methods: This study included 44 patients with skeletal Class III malocclusion who underwent Le Fort I osteotomy and BSSRO for mandibular SB. The patients in the experimental group (BSSRO with ASO; n = 11) and the control group (BSSRO without ASO; n = 33) were compared statistically for the amount of surgical movement and changes in the PAS using computed tomography (CT). In experimental group, 7 patients underwent palatal expansion and 3 patients underwent maxillary ASO. Both the experimental and control groups were divided into two subgroups (Groups A and B) according to the SB amount of the second molar (Group A: SB < 10 mm; Group B: SB ≥ 10 mm). Simulations of airflow velocity and negative pressure in the PAS were analyzed using computational fluid dynamics.

Results: In experimental group, patients with maxillary ASO showed the forward movement of #7 tooth was 2.5mm at crown. The cross-sectional area of PNS increased by 28% and Nasopharynx volume increased by 33.67%. Patients with palatal expansion showed average expansion amount of 6.56mm at crown. The cross-sectional area of PNS increased by 21.95% and Nasopharynx volume increased by 26.39%. The efficiency of mandibular ASO in decreasing mandibular SB movement in the experimental group was 7.01 ± 2.38 mm at the cusp tip and 6.46 ± 2.26 mm at the root apex of the canine. In Group A, the cross-sectional area at the level of the posterior nasal spine and the soft palate and the volume of the upper and middle PAS revealed a significant decrease in the control group and a significant increase in the experimental group ($p < 0.05$). In Group B, the transversal length at the level of the soft palate and the volume of the middle PAS decreased in the control group and increased in the experimental group. The upper PAS volume was increased in both groups while being more enlarged in the experimental group ($p < 0.05$). In Group B, maximum air velocity significantly decreased in the experimental group, whereas it increased in the control group ($p < 0.05$). In Group A, the decrease in the experimental group and increase in the control group were not significant.

Conclusions: Maxillary ASO is more effective than palatal expansion in clearing the airway in Nasopharynx. The present study demonstrates that mandibular ASO combined with BSSRO is an effective surgical method for reducing the amount of mandibular SB movement and decreasing the PAS reduction in patients with mandibular prognathism. This method improves the airflow dynamics compared with BSSRO SB without ASO. Additional PSG analysis is needed to evaluate whether BSSRO SB with ASO can suppress OSA

Keywords : mandibular prognathism, mandible setback, anterior segmental osteotomy, pharyngeal airway, computational fluid dynamics

Student Number : 2017-39152

CONTENTS

I. Introduction

Mandibular setback (SB) with bilateral sagittal split ramus osteotomy (BSSRO) has been used frequently for the improvement of skeletal malocclusion and facial profile in patients with mandibular prognathism. In this surgery, surgical movement changes the position of the jaws and soft tissue to achieve adequate maxillomandibular relationship and esthetics, but this may also cause changes in the pharyngeal airway space (PAS) by pushing and stretching the soft tissue [1, 2].

Many studies have evaluated the changes in the PAS after BSSRO for mandibular SB movement. As the mandible moves backward, the volume of the airway space may decrease [3, 4] due to the posterior displacement of the tongue and soft palate (Figure 1) [5, 6]. There has been some variety in the results of research investigating the volume of the PAS after mandibular SB surgery. However, the majority of the studies have shown that the space has narrowed [7–11], despite the fact that after bimaxillary surgery, it has in some cases remained unchanged [1, 12–16] or increased [17]. Patients who have narrow PAS preoperatively, or undergo a large amount of mandibular SB movement, may suffer from obstructive sleep apnea (OSA) or snoring due to the airway space reduction [2, 18–20]. In a study by Jang et al. on PAS changes after mandibular SB surgery, the oropharyngeal airway volume was reduced by 29%, whereas the upper airway space and hypopharyngeal volume also decreased, and the apnea-hypopnea index (AHI) increased (although the increase in index was not statistically significant) [21]. Guilleminault et al. first reported the development of OSAS in two patients who underwent mandibular SB surgery for the treatment of mandibular prognathism [22]. Hasebe et al. further presented two patients who developed postoperative OSA after a more than 12–13-mm mandibular SB [23]. Yang et al. also evaluated the effect of large mandibular SB (>9 mm) on postoperative changes in the PAS using 3-dimensional (3D) computed tomography (CT), as well as changes in polysomnography (PSG) parameters in relation with the occurrence of OSA [24]. In their study, 33.3% of patients with a large amount of mandibular SB had newly developed OSA.

On the basis of these previous studies, the risk of OSA should be considered in the surgical planning for patients undergoing surgery that includes a large mandibular SB. For these patients, considering a change in surgical methods is necessary in order to minimize the PAS reduction caused by surgery. First, maxillary advancement should be considered, because it is able to reduce the amount of mandibular SB and increase the PAS. Mucedero et al. [25] analyzed the change in pre- and post-treatment parameters in the lateral cephalometric radiograph of patients in two groups who had undergone maxillary advancement using a facemask/bite block with rapid palatal expansion (RPE). In this study, the anteroposterior length of the PAS was increased after treatment. Cakirer et al. [26] further analyzed the upper airway changes in the lateral cephalogram in patients who had undergone maxillary advancement using Le Fort I osteotomy or orthodontic treatment using RPE or a facemask. In this study, there was a statistically significant increase in the nasopharyngeal area in both groups, but no significant change in the oropharyngeal cavity volume. However, maxillary advancement in Northeast Asian patients with flat mid-face profile and a small nose may cause unwanted facial esthetics, namely, a protrusive upper lip and upturned nose. Therefore, the amount of possible maxillary advancement is limited, and a large amount of mandibular SB is inevitably favored for esthetic reasons in Korea [27, 28].

A second alternative surgical approach is mandibular SB surgery combined with anterior segmental osteotomy (ASO; Figures 2 and 3). The main principle of this technique is to maintain the amount of backward movement of the anterior mandibular segment while reducing the amount of backward movement of the posterior mandibular segment by the closure of extraction space in the mandibular premolar after ASO. The theory of this method is based on a report by Goh and Lim [29], in which problems regarding unacceptable esthetic alterations and decreased long-term stability of advanced skeletal segments were solved by combining ASO with the classic maxillomandibular advancement (MMA) surgery.

Although mandibular SB surgery combined with ASO could reduce the decrease in PAS in a case analysis (Figure 4), a study using statistical analysis has not yet been undertaken with regard to whether this surgical method actually reduces the amount of posterior mandible SB. Han et al. [30] reported two cases of surgical maxillary expansion and mandibular SB with ASO used to treat mandibular prognathism with OSA. However, there has been no comparative study between this alternative method and the conventional method using BSSRO only to evaluate the effect of ASO on changes in the PAS after mandibular SB surgery.

Polysomnography (PSG) is a standard tool used for the assessment of respiratory disturbances, including a patient's quality and quantity of sleep. PSG has also been used to measure patients' physiological characteristics after mandibular SB surgery [16, 23, 31, 32]. However, PSG needs to be performed overnight twice, before and after orthognathic surgery, and is an expensive process; patients may hesitate to participate in examinations in an unfamiliar laboratory environment [16, 23, 31, 32]. Another tool for the assessment of respiratory disturbance after mandibular SB surgery is computational fluid dynamics (CFD), in which a virtual simulation is created for the purpose of studying airflow. The narrowest area of the PAS is considered to be important for respiratory disturbance [33] because the degree of the PAS contraction is the most important factor in the development of airflow resistance, according to Poiseuille's law [33]. Some researchers have emphasized that changes in the minimum axial area of the PAS may be more important than those in the total volume [34, 35]. Accordingly, CFD is currently being used to analyze the airflow dynamics of the upper airway [36–41]. With CFD, irregular turbulent characteristics under certain boundary conditions can be calculated using an algorithm [42]. The advantages of CFD also include ease of observation and the prediction of fluid flows that are otherwise difficult to discern [43]. Despite a lack of comprehensive information regarding the respiration process [44], the characteristics of airflow in the upper airway have become a major area of interest when studying patients with sleep disorder [45, 46]. Kim et al. [47] compared the changes in the PAS using 3D CFD analysis in two patients with OSA, one who had undergone conventional MMA and one who had undergone modified MMA with ASO. In their study, the maximum velocity of airflow had decreased in both patients, whereas AHI improved from 61.0 to 6 in the modified MMA patient and from 43.2 to 15.2 in the conventional

MMA patient.

Although, theoretically, ASO combined with BSSRO for mandibular SB may reduce the amount of mandibular SB and prevent PAS narrowing, as of yet, there has been no report on the level of reduction in mandibular SB movement achieved by combining ASO with BSSRO in patients with mandibular prognathism. Also, there has been no comparative study using statistical analysis concerning the effect of ASO on the reduction of PAS narrowing; even though CFD has been used for the evaluation of the airway space, there has been no comparative CFD analysis regarding the respiration airway flow of patients with mandibular SB surgery using ASO combined with BSSRO and patients with BSSRO only.

This study aimed to evaluate the efficacy of ASO in the reduction of mandibular SB in patients undergoing mandibular SB surgery. The effect of ASO combined with BSSRO compared with BSSRO without ASO on the reduction of PAS narrowing was also evaluated. The airflow dynamics were analyzed using CFD in 3D CT based on pre- and postoperative PAS.

II. Materials and methods

2.1. Patients

This study included 44 patients (25 males and 19 females) who had skeletal class III malocclusion and were treated with bimaxillary orthognathic surgery (BSSRO and Le Fort I osteotomy). The average age of the patients was 24.0 ± 5.23 years old.

The experimental group was composed of 11 patients (6 males and 5 females; average age = 25.6 ± 6.44 years old) with mandibular prognathism who underwent surgical correction using BSSRO combined with ASO and Le Fort 1 osteotomy, with or without genioplasty (Table 1). Three surgical methods were used to compensate for the maxillary transversal discrepancy that had occurred due to the mandibular ASO. The first method was maxillary ASO (n = 3; Figure 5), the second was maxillary palatal expansion (n = 7; Figures 6 and 7), and the last was orthodontic treatment (n = 1). The patients who underwent glossectomy and who had mandibular ASO due to orthodontic needs were excluded.

The control group consisted of 33 patients (19 males and 14 females;

average age = 23.5 ± 4.76 years old). Three patients who had a similar amount of mandibular SB movement to the 11 patients in the experimental group were matched to those in the experimental group via the following procedure to reduce individual variation of the PAS in the control group: (1) the virtual mandibular SB of patients in the experimental group were calculated if ASO had not been performed, and (2) three patients who underwent bimaxillary surgery without mandibular ASO and who had approximately the same amount of virtual mandibular SB as those in the experimental group were selected.

The preoperative median body mass index (BMI) of patients in the experimental group (23.87 ± 3.22 kg/m2) and the postoperative BMI of these patients (23.37 ± 2.83 kg/m2) were not significantly different. The median BMI of patients in the control group (21.76 ± 3.33 kg/m2) had significantly decreased after surgery (22.11 ± 3.16 kg/m2; $p = 0.038$).

1.2. Acquisition and transformation of CT images

3D facial CT scans of all patients were obtained using a CT scanner

(Siemens SOMATOM sensation 10, Munich, Germany) with the following parameters: 120 kVp; 80 mAs; slice thickness = 0.75 mm. CT scans were taken before (T0) and 3 to 6 months after surgery (T1). Digital image files were exported in a Digital Imaging and Communications in Medicine (DICOM) format and imported into On Demand 3D® (Cybermed, Seoul, Korea) and Invivo Dental software® (Anatomage, San Jose, CA). To standardize the measurements and to minimize errors, a Frankfort horizontal (FH) plane was constructed for reorientation of the 3D images.

1.3. Evaluation of the effect of maxillary ASO, palatal expansion and mandibular SB reduction in ASO combined with BSSRO

Computed tomography images at different time points (T0 and T1) were taken at the cranial base and superimposed using On Demand 3D® (Cybermed, Seoul, Korea). A 3D coordinate system was established (X: medial–lateral; Y: anterior–posterior; Z: superior–inferior). The FH plane, which passed through the left and right orbitals and right porion, was used as a horizontal reference plane. The nasion landmark was used as the origin

(0, 0, 0). According to the manufacturer's recommended protocol, the X-axis was set as a vector from the right orbital to the left orbital, and the midsagittal plane was defined as the plane perpendicular to the X-axis and passing through the nasion. The surgical movements of the maxilla and mandible were measured in the CT images according to the movement of the mandibular ASO segment and the movement of the maxilla and distal mandibular segments. To measure the direction and amount of segmental movement after ASO, the anteroposterior and superoinferior changes of the B point, lower central incisor/canine crown tip and lower central incisor/canine root tip, were calculated. For the maxillary movement, the anteroposterior and superoinferior changes of the A point, the distobuccal (DB) cusp and the palatal root tip of the upper second molar (#7), were calculated. The movement of the mandible was obtained by calculating the anteroposterior and superoinferior changes of the lower #7 DB cusp and distal root tip. The efficacy of the ASO was obtained by calculating the difference in SB amount between the canine and the second molar on both maxilla and mandible. The amount of palatal expansion was obtained by calculating the difference in left-right movement of maxillary right and left #7 crown and palatal root tip.

1.4. Evaluation of the effect of additional osteotomies on the reduction of PAS narrowing

The PAS was evaluated for changes in distance and area as well as for changes in airway volume using CT and axial CT, respectively.

2.4.1 Changes in distance and cross-sectional area at three vertical levels

The PAS was investigated at T0 and T1 at the three vertical levels listed below [Figure 8-A]:

(1) The posterior nasal spine (PNS) parallel to the FH plane.

(2) The most posterior point of the soft palate (SP) parallel to the FH plane.

(3) The most posterior point of the tongue base (TB) parallel to the FH plane.

At each of these three levels, the highest transverse width (MD), the anteroposterior length (AP), and the cross−sectional area (CSA) were also measured.

2.4.2. Changes in airway volume

Digital image files were exported in a Digital Imaging and Communications in Medicine (DICOM) format and imported into Invivo Dental software® (Anatomage, San Jose, CA). These images were rendered into volumetric images of the PAS. The sagittal, axial, and coronal planes were reconstructed, and 3D models were obtained. To standardize the measurements and minimize errors, the FH plane was constructed for reorientation of the 3D images. The FH plane was constructed from the right and left porions and right orbital. To determine the volume of the airway, the threshold value was set at a range of −1,024 to −600 Hounsfield units. The airway was divided into three regions using hard tissue references as follows [Figure 8−B]:

(1) PNS−Vp plane: perpendicular to the midsagittal plane passing through PNS and the posteriormost part of the ala of vomer (Vp).

(2) CV1 (first cervical vertebrae) plane: parallel to the FH plane passing through the inferiormost point of CV1.

(3) CV2 plane: parallel to the FH plane passing through the inferiormost point of CV2.

(4) CV4 plane: parallel to the FH plane passing through the inferiormost point of CV4.

The airway was divided into three regions relative to the reference planes as follows:

(1) Nasopharyngeal volume (V1) between the PNS−Vp and CV1 plane.

(2) Oropharyngeal volume (V2) between the CV1 and CV2 planes.

(3) Hypopharyngeal volume (V3) between the CV2 and CV4 planes.

The PASs in CT were measured by the same examiner at T1 and T2 in all patients using Invivo Dental software® (Anatomage, San Jose, CA). The airway change parameters (length, width, CSA, and volume) were described by absolute values and rate (%). The rate was calculated using the following formula:

$$Rate\ (\%) = \frac{(\mathrm{T2} - \mathrm{T0})}{\mathrm{T0}} * 100$$

2.5. Analysis of respiratory airway flow using CFD

The patients for whom CT revealed a completely obstructed airway at T0 or T2 (two patients in the experimental group; one patient in the control group) were excluded from the analysis. The Mimics program (Materialise, Leuven, Belgium) and Midas NFX CFD® (Midas IT, Seongnam, Korea) were used to analyze airflow dynamics.

2.5.1. Geometrical modeling and meshing

Digital image files were exported in a DICOM format and imported into the Mimics program commercial software (Materialise, Leuven, Belgium). These images were then used to construct individualized 3D airway models as follows: (1) the boundary condition was set on the 3D-CT images, and a threshold level of −1024 to −200 was applied to the area consisting of air; (2) the boundary lines or contours on the 3D-CT images were set using the laminating method; (3) finally, after the surface model had been smoothed and stored in the stereolithography file format (Figure 9), it was imported using a commercial mesh generation software, Midas NFX CFD® (Midas IT, Seongnam, Korea). Then, the mesh was generated with tetrahedron and prism elements (Figure 10).

2.5.2. Numerical analysis

For the computer simulation of airflow, the flow was assumed to be incompressible. To account for the possible existence of turbulence, the Reynolds-averaged Navier-Stokes equation was solved for the turbulent flow, and the K-epsilon (k-ε) turbulence model was also used. The k-ε model approximation was sufficient to depict the low-scale swirling in the upper airway with affordable computational effort and the ability to predict pressure changes and velocity distributions of the respiratory flow.

2.5.2.1. Numerical method and variables

Numerical analysis was conducted using a commercial CFD package, Midas NFX CFD® (Midas IT, Seongnam, Korea) based on the finite volume method. A 3D transient state incompressible turbulent airway field was obtained by solving continuity and Navier–Stokes equations computationally. A constant air density of 1.08 kg/m3 and a constant air temperature of 25 ℃ were assumed. No-slip wall boundary conditions were imposed on the airway walls. The boundary condition at the nostril of an inlet was set to the following respiration cycle: 34.3 L/min (peak of inspiration), −2.5 L/min (end of the expiration), and −29.5 L/min (peak of expiration) [48]. Midas NFX CFD® (Midas IT, Seongnam, Korea) was used to measure the maximum airflow velocity and peak negative pressure [Figure 11].

2.6. Statistical evaluation

Descriptive statistics included the mean and the standard deviation, with a 95% confidence interval for both the mean and median. Statistical analysis was conducted using SPSS Version 25 for Windows (IBM, Chicago, IL, USA). The Wilcoxon signed-rank test and the Mann–Whitney U test were used to determine significance. Differences were considered to be significant at $p < 0.05$.

III. Results

3.1. Evaluation of amount of palatal expansion and maxillary ASO

In experimental group, the efficacy of space closure by maxillary ASO after extraction of first premolar (n = 3) was 7 mm at crown, while it was only 1.5mm at root. The forward movement of #7 tooth was 2.5mm at crown and 2.6mm at root. In PAS at the PNS level, the anterior−posterior length of the cross−section increased by 23.59%, but the width decreased by 2.2%. The cross−sectional area at the PNS level increased by 28%, and the nasopharynx volume increased by 33.67%, as presented in Table 2. The average amount of palatal expansion after maxillary mid−palatal osteotomy (n = 7) was 6.56mm at crown and 5.25mm at root. In PAS at the PNS level, the anterior−posterior length of the cross section increased by 19.19% and the width increased by 3.57%. The cross−sectional area at the PNS level increased by 21.95%, and the nasopharynx volume increased by 26.39%, as presented in Table 2.

The results showed that maxillary ASO was more effective than palatal expansion to enlarge the airwayin nasopharynx.

3.2. Evaluation of reduced mandibular SB movement in ASO combined with BSSRO

As presented in Table 3, the mean maxillary advancement at A point was 0.35 ± 2.53 mm in the experimental group and 1.07 ± 1.87 mm in the control group. The mean mandibular SB at B point was 12.94 ± 5.93 mm in the experimental group and 10.04 ± 3.01 mm in the control group. It follows that differences in maxillary advancement between the experimental group and control group were not statistically significant ($p > 0.05$). The mandibular SB at the DB cusp of the second molar was only 5.13 ± 6.33 mm in the experimental group, this being significantly less than that in the control group (10.52 ± 2.76 mm; $p = 0.008$). The efficiency of ASO in the experimental group was 7.01 ± 2.38 mm at cusp tip and 6.46 ± 2.26 at root tip, as presented in Table 4.

3.3. Evaluation of the effect of ASO on the reduction of PAS narrowing

3.3.1. Postoperative airway changes in all patients

In the comparison between preoperative and postoperative airway parameters, the anterior–posterior and transverse distances at the level of the soft palate (AP_SP, p = 0.014; TRV_SP, p = 0.002) and the tongue base (AP_TB, p = 0.000; TRV_TB, p = 0.012) were significantly reduced in the control group after surgery. Meanwhile, the anterior–posterior distances at the level of the PNS (AP_PNS; p = 0.041) had not significantly increased, or reduced in the experimental group, whereas at the level of the tongue base (AP_TB; p = 0.021), the anterior–posterior distances significantly decreased. In terms of the CSA and volume, the control group exhibited a significant reduction in the CSA at the level of the soft palate (p = 0.002) and the tongue base (p = 0.000), as well as in V2 (p = 0.000) and V3 (p = 0.002), whereas the experimental group presented a significant increase in V1 (p = 0.006). Even though there was no significant increase, the CSA at the level of the PNS and soft palate, as well as V2, increased after surgery in the experimental group. These results are summarized in Table 5.

3.3.2. Postoperative airway changes in subgroups

In Group A (mandibular SB < 10 mm), there were significant differences between the experimental and control groups in CSA_PNS ($p = 0.03$), CSA_SP ($p = 0.01$), V1 ($p = 0.05$), and V2 ($p = 0.01$). All four parameters decreased in the control group and increased in the experimental group. In Group B (mandibular SB ≥ 10 mm), there were significant differences between the experimental and control groups in TRV_SP ($p = 0.01$), V1 ($p = 0.03$), and V2 ($p = 0.05$). With respect to TRV_SP and V2, there was a decrease in the control group and an increase in the experimental group. With respect to V1, both the control and the experimental groups exhibited an increase, but the increase in V1 was greater in the experimental group than in the control. These results are summarized in Table 6 and Figure 12.

3.4. Respiration airway flow using CFD

In Group A, the maximum airflow velocity decreased in the experimental group and increased in the control group, without statistical significance. In the experimental group of Group B, the maximum air velocity was significantly decreased at the end of expiration ($p = 0.018$) and at the peak of expiration ($p = 0.016$) compared with that of the control group. In the experimental group of Group B, the peak negative pressure was also significantly decreased at the end of expiration ($p = 0.013$) and at the peak of expiration ($p = 0.013$), whereas these parameters were increased in the control group. These results are summarized in Table 7 and Figure 13.

IV. Discussion

Maxillary advancement, maxillary expansion, and maxillomandibular advancement have a definite effect on the improvement of symptoms in sleep apnea patients. Riley et al. [49] reviewed 40 patients who underwent soft tissue and skeletal surgery for sleep apnea, of whom 36 (90%) experienced long-term improvement. In particular, respiratory disturbance index (RDI) significantly decreased ($p < 0.01$) in MMA patients. However, considering the facial appearance of Northeast Asian people, in particular, the prominent upper lip and small nose, the amount of maxillary advancement should be limited to avoid undesirable esthetic impairment [27, 28]. In order to perform a sufficient amount of MMA without negatively impacting facial aesthetics, Goh et al. [29] introduced a modified MMA, in which the ASO of the upper and lower jaws was combined with MMA. Using this method, the PAS can also be increased due to the forward movement of the upper and lower bone fragments while reducing the protrusion of the anterior lip. Evaluation using polysomnography and clinical photographs of 11 patients who underwent modified MMA revealed that sleep apnea indicators improved dramatically.

Based on this theory, an SSRO that combines maxillary and mandibular ASO was devised. In this procedure, after mandibular SB movement, the position of the mandibular anterior segment is maintained, whereas the posterior part of the distal segment is moved to the premolar extraction space, thereby improving the facial appearance and simultaneously reducing the amount of distal segment SB [30]. Because the premolar diameter is approximately 7 mm on average, it is possible to reduce the amount of mandibular SB up to 6–7 mm. Theoretically, in patients requiring 10 mm of mandibular SB to obtain an acceptable esthetic appearance, the amount of SB can be reduced to 3–4 mm. This may also reduce PAS narrowing and the risk of postoperative sleep apnea. According to our results, the efficiency of ASO was 7.01 ± 2.38 mm at cusp tip and 6.46 ± 2.26 mm at root apex, which demonstrates that the premolar space can be fully utilized. Moreover, in some patients, the efficiency of ASO was more than 7 mm, which is far greater than the average size of the premolar tooth. This level of efficiency can also be obtained by lingual tilting of the anterior segment.

In mandibular ASO, the anterior segment may not move parallel to the occlusal surface but may tilt towards the labial or lingual side (Figures 14 and 15). Tilting the ASO segment to the lingual side reduces the SB of the cusp tip even more by eliminating the bumps between the roots. In our study, the efficiency at the crown level was greater than that at the root level, which explains the lingualization of the anterior segment.

During mandibular ASO, moving the ASO segment backward creates an imbalance in the mandibular arch form. This imbalance should be resolved by moving the second premolar and the canine inward. Thus, it is recommended that 1 mm of the leeway space for each mesial and distal sides of the extracted premolar should be maintained for post−operative orthodontic treatment. Considering this space (the actual available space is only about 5 mm), the lingualization of the anterior segment is helpful as a surgical maneuver to increase the level of SB of the anterior segment into the extracted premolar space.

The increase in nasopharyngeal and oropharyngeal airway volumes after mandibular SB surgery in the experimental group appeared to be caused by the maxillary expansion. In cases of mandibular ASO, cross−bite usually occurs in the posterior region after establishing the ideal anteroposterior relationship between the upper and lower incisors. In these cases, this discrepancy can be eliminated by performing maxillary ASO or maxillary expansion. In our study, seven patients in the experimental group underwent palatal expansion. It has been reported that palatal expansion induces lateral expansion of the airway space; the increase in PAS following palatal expansion can be inferred from previous studies in which there was an increase in airway space after RPE [50]. In a study of airway space using a lateral cephalogram, an increase in the cross−sectional area of the nasopharyngeal airway was observed after RPE [50]. Unfortunately, a significant increase in the oropharyngeal volume after RPE was not reported in previous studies [19, 51, 52]. Because of anatomical distance, the oropharyngeal airway is less affected by RPE than the nasopharyngeal airway [30, 52]. Izuka et al. [53] reported an increased volume of the oropharyngeal cavity by 1450.6 mm3 after RPE and an improved breathing even though the increase was not significant. Widening of the airway space was also reported after additional palatal expansion with orthognathic surgery [11, 16]. Han et al. [30] reported two patients with mandibular prognathism and OSA who underwent two jaw surgeries with simultaneous maxillary expansions. In these cases, airway volume was maintained or increased, and polysomnography (PSG) parameters related to sleep apnea were improved.

When evaluating the risk of sleep apnea, it is necessary to evaluate respiratory disturbance using PSG. The AHI, which is the average number of obstructive apneas and hypopneas per hour, can determine the severity of OSA [54]. PSG is an effective tool, but it requires a significant time investment [55] and requires patients to stay overnight, making it a slow and expensive process. Thus, PSG is usually accessible for only a small portion of the population. A simplified version of PSG [56, 57] has thus been developed to improve accessibility of the process [58, 59]. Recently, 3D CFD analysis has also been used to simulate the laminar and turbulent airflow through the posterior–superior airway and to analyze airflow in OSA patients [60–62]. Kim et al. [47] analyzed airflow by extracting 3D airway space models from the CT data of two patients, one who underwent conventional MMA and one who underwent modified MMA. With regard to the respiratory parameters in the PSG of both patients, a decrease in airflow velocity was observed in CFD. Yajima et al. [63] used CFD to investigate the relationship between the pressure drop in the pharyngeal airway space and the minimum cross-sectional area of the pharyngeal airway in 11 patients before and after mandibular SB surgery. When the minimum cross-sectional area was <1 cm2, the pressure drop increased greatly, leading to an increased risk of postoperative OSA after surgery. However, CFD analysis alone cannot assess OSA, because OSA cannot be evaluated by the anatomical shape or volume of the airway space alone but must be evaluated with a continuous observation of neuromuscular reaction. Further development and improvement in the simulated movement of the pharyngeal soft tissue in CFD may provide functional prediction of PAS changes and respiratory disturbances after mandibular SB movement.

.

V. Conclusion

Using ASO, the amount of mandible SB can be reduced by 7 mm on average. Using ASO combined with BSSRO, PAS narrowing after mandibular SB surgery can also be reduced. In the fluid dynamics study, mandibular SB with BSSRO combined with ASO was demonstrated to improve the airflow dynamics compared with BSSRO SB without ASO. Additional PSG analysis is needed to evaluate whether BSSRO SB with ASO can suppress OSA

VI. References

1. Hatab, N.A., V.S. Konstantinovic, and J.K. Mudrak, *Pharyngeal airway changes after mono- and bimaxillary surgery in skeletal class Ⅲ patients: Cone-beam computed tomography evaluation.* J Craniomaxillofac Surg, 2015. **43**(4): p. 491-6.
2. Lye, K.W., *Effect of orthognathic surgery on the posterior airway space (PAS).* Ann Acad Med Singapore, 2008. **37**(8): p. 677-82.
3. Turnbull, N.R. and J.M. Battagel, *The effects of orthognathic surgery on pharyngeal airway dimensions and quality of sleep.* J Orthod, 2000. **27**(3): p. 235-47.
4. Enacar, A., et al., *Changes in hypopharyngeal airway space and in tongue and hyoid bone positions following the surgical correction of mandibular prognathism.* Int J Adult Orthodon Orthognath Surg, 1994. **9**(4): p. 285-90.
5. Katsantonis, G.P., et al., *Determining the site of airway collapse in obstructive sleep apnea with airway pressure monitoring.* Laryngoscope, 1993. **103**(10): p. 1126-31.
6. Boudewyns, A.N., P.H. Van de Heyning, and W.A. De Backer, *Site of upper airway obstruction in obstructive apnoea and influence of sleep stage.* Eur Respir J, 1997. **10**(11): p. 2566-72.
7. Brunetto, D.P., et al., *Prediction of 3-dimensional pharyngeal airway changes after orthognathic surgery: a preliminary study.* Am J Orthod Dentofacial Orthop, 2014. **146**(3): p. 299-309.
8. Hong, J.S., et al., *Three-dimensional changes in pharyngeal airway in skeletal class Ⅲ patients undergoing orthognathic surgery.* J Oral Maxillofac Surg, 2011. **69**(11): p. e401-8.
9. Kim, M.A., et al., *Three-dimensional changes of the hyoid bone and airway volumes related to its relationship with horizontal anatomic planes after bimaxillary surgery in skeletal Class Ⅲ patients.* Angle Orthod, 2013. **83**(4): p. 623-9.
10. Li, Y.M., et al., *Morphological changes in the pharyngeal airway of female skeletal class Ⅲ patients following bimaxillary surgery: a cone beam computed tomography evaluation.* Int J Oral Maxillofac Surg, 2014. **43**(7): p. 862-7.
11. Shin, J.H., et al., *A 2-year follow-up of changes after bimaxillary surgery in patients with mandibular prognathism: 3-dimensional analysis of pharyngeal airway volume and hyoid bone position.* J Oral Maxillofac Surg, 2015. **73**(2): p. 340 e1-9.
12. Hart, P.S., et al., *Postsurgical volumetric airway changes in 2-jaw orthognathic*

surgery patients. Am J Orthod Dentofacial Orthop, 2015. **147**(5): p. 536-46.

13. Jakobsone, G., L. Neimane, and G. Krumina, *Two- and three-dimensional evaluation of the upper airway after bimaxillary correction of Class Ⅲ malocclusion.* Oral Surg Oral Med Oral Pathol Oral Radiol Endod, 2010. **110**(2): p. 234-42.
14. Lee, Y., et al., *Volumetric changes in the upper airway after bimaxillary surgery for skeletal class Ⅲ malocclusions: a case series study using 3-dimensional cone-beam computed tomography.* J Oral Maxillofac Surg, 2012. **70**(12): p. 2867-75.
15. Park, S.B., et al., *Cone-beam computed tomography evaluation of short- and long-term airway change and stability after orthognathic surgery in patients with Class Ⅲ skeletal deformities: bimaxillary surgery and mandibular setback surgery.* Int J Oral Maxillofac Surg, 2012. **41**(1): p. 87-93.
16. Uesugi, T., et al., *Effects of orthognathic surgery on pharyngeal airway and respiratory function during sleep in patients with mandibular prognathism.* Int J Oral Maxillofac Surg, 2014. **43**(9): p. 1082-90.
17. Gokce, S.M., et al., *Changes in posterior airway space, pulmonary function and sleep quality, following bimaxillary orthognathic surgery.* Int J Oral Maxillofac Surg, 2012. **41**(7): p. 820-9.
18. Chen, F., et al., *Effects of bimaxillary surgery and mandibular setback surgery on pharyngeal airway measurements in patients with Class Ⅲ skeletal deformities.* Am J Orthod Dentofacial Orthop, 2007. **131**(3): p. 372-7.
19. Cho, H.W., et al., *Retrospective study of changes in pharyngeal airway space and position of hyoid bone after mandibular setback surgery by cephalometric analysis.* Maxillofac Plast Reconstr Surg, 2015. **37**(1): p. 38.
20. Kitahara, T., et al., *Changes in the pharyngeal airway space and hyoid bone position after mandibular setback surgery for skeletal Class Ⅲ jaw deformity in Japanese women.* Am J Orthod Dentofacial Orthop, 2010. **138**(6): p. 708 e1-10; discussion 708-9.
21. Jang, S.I., et al., *Three-dimensional analysis of changes in airway space after bimaxillary orthognathic surgery with maxillomandibular setback and their association with obstructive sleep apnea.* Maxillofac Plast Reconstr Surg, 2018. **40**(1): p. 33.
22. Guilleminault, C., R. Riley, and N. Powell, *Sleep apnea in normal subjects following mandibular osteotomy with retrusion.* Chest, 1985. **88**(5): p. 776-8.
23. Hasebe, D., et al., *Changes in oropharyngeal airway and respiratory function during*

sleep after orthognathic surgery in patients with mandibular prognathism. Int J Oral Maxillofac Surg, 2011. **40**(6): p. 584-92.

24. Yang, H.J., et al., *Airway changes and prevalence of obstructive sleep apnoea after bimaxillary orthognathic surgery with large mandibular setback.* Int J Oral Maxillofac Surg, 2019.

25. Mucedero, M., et al., *Effects of maxillary protraction with or without expansion on the sagittal pharyngeal dimensions in Class III subjects.* Am J Orthod Dentofacial Orthop, 2009. **135**(6): p. 777-81.

26. Cakirer, B., et al., *Sagittal airway changes: rapid palatal expansion versus Le Fort I osteotomy during maxillary protraction.* Eur J Orthod, 2012. **34**(3): p. 381-9.

27. Ahn, H.W., et al., *Surgical treatment modality for facial esthetics in an obstructive sleep apnea patient with protrusive upper lip and acute nasolabial angle.* Angle Orthod, 2013. **83**(2): p. 355-63.

28. Ahn, H.W., et al., *Stability of Modified Maxillomandibular Advancement Surgery in a Patient With Preadolescent Refractory Obstructive Sleep Apnea.* J Oral Maxillofac Surg, 2015. **73**(9): p. 1827-41.

29. Goh, Y.H. and K.A. Lim, *Modified maxillomandibular advancement for the treatment of obstructive sleep apnea: a preliminary report.* Laryngoscope, 2003. **113**(9): p. 1577-82.

30. Han, J.J., D.H. Hong, and S.J. Hwang, *Maxillary Expansion and Mandibular Setback Surgery With and Without Mandibular Anterior Segment Osteotomy to Correct Mandibular Prognathism With Obstructive Sleep Apnea.* J Craniofac Surg, 2017. **28**(3): p. 723-730.

31. Demetriades, N., et al., *Effects of mandibular retropositioning, with or without maxillary advancement, on the oro-naso-pharyngeal airway and development of sleep-related breathing disorders.* J Oral Maxillofac Surg, 2010. **68**(10): p. 2431-6.

32. Hochban, W., et al., *Mandibular setback for surgical correction of mandibular hyperplasia--does it provoke sleep-related breathing disorders?* Int J Oral Maxillofac Surg, 1996. **25**(5): p. 333-8.

33. Tepecik, T., U. Ertas, and M. Akgun, *Effects of bimaxillary orthognathic surgery on pharyngeal airway and respiratory function at sleep in patients with class III skeletal relationship.* J Craniomaxillofac Surg, 2018. **46**(4): p. 645-653.

34. Haskell, J.A., et al. *Effects of mandibular advancement device (MAD) on airway dimensions assessed with cone-beam computed tomography.* in *Seminars in*

Orthodontics. 2009. Elsevier.
35. Lenza, M.G., et al., *An analysis of different approaches to the assessment of upper airway morphology: a CBCT study.* Orthod Craniofac Res, 2010. **13**(2): p. 96-105.
36. Bates, A.J., et al., *Assessing the relationship between movement and airflow in the upper airway using computational fluid dynamics with motion determined from magnetic resonance imaging.* Clinical Biomechanics, 2017.
37. Ephros, H.D., et al., *Developing a protocol for the surgical management of snoring and obstructive sleep apnea.* Atlas of the oral and maxillofacial surgery clinics of North America, 2007. **15**(2): p. 89-100.
38. Dailey, H.L. and S. Ghadiali, *Fluid-structure analysis of microparticle transport in deformable pulmonary alveoli.* Journal of Aerosol Science, 2007. **38**(3): p. 269-288.
39. Soose, R.J., *Novel surgical approaches for the treatment of obstructive sleep apnea.* Sleep medicine clinics, 2016. **11**(2): p. 189-202.
40. Chouly, F., et al., *Numerical and experimental study of expiratory flow in the case of major upper airway obstructions with fluid–structure interaction.* Journal of Fluids and Structures, 2008. **24**(2): p. 250-269.
41. Sun, X., et al., *Numerical simulation of soft palate movement and airflow in human upper airway by fluid-structure interaction method.* Acta Mechanica Sinica, 2007. **23**(4): p. 359-367.
42. Majumdar, P., *Computational fluid dynamics analysis of turbulent flow.* 2011: Intech.
43. Ruiz, P.C., et al., *Computational fluid dynamics simulations of the airflow in the human nasal cavity.* Acta otorrinolaringologica espanola, 2005. **56**(9): p. 403.
44. Pirnar, J., et al., *Computational fluid-structure interaction simulation of airflow in the human upper airway.* Journal of biomechanics, 2015. **48**(13): p. 3685-3691.
45. Barrera, J.E., *Skeletal Surgery for Obstructive Sleep Apnea.* Sleep Med Clin, 2018. **13**(4): p. 549-558.
46. Gupta, R.J., D. Kademani, and S.Y. Liu, *Upper Airway (Hypoglossal Nerve) Stimulation for Treatment of Obstructive Sleep Apnea.* Atlas Oral Maxillofac Surg Clin North Am, 2019. **27**(1): p. 53-58.
47. Kim, T., et al., *Change in the Upper Airway of Patients With Obstructive Sleep Apnea Syndrome Using Computational Fluid Dynamics Analysis: Conventional Maxillomandibular Advancement Versus Modified Maxillomandibular Advancement With Anterior Segmental Setback Osteotomy.* J Craniofac Surg, 2015. **26**(8): p. e765-70.

48. Scurr, C. and S.A. Feldman, *Scientific foundations of anaesthesia*. 3rd ed. 1990, Chicago: Distributed by Year Book Medical Publishers. xv, 643 p.
49. Riley, R.W., et al., *Surgery and obstructive sleep apnea: long-term clinical outcomes.* Otolaryngol Head Neck Surg, 2000. **122**(3): p. 415-21.
50. Basciftci, F.A., et al., *Does the timing and method of rapid maxillary expansion have an effect on the changes in nasal dimensions?* Angle Orthod, 2002. **72**(2): p. 118-23.
51. Ho, M.W., et al., *Surgical complications of segmental Le Fort I osteotomy.* Br J Oral Maxillofac Surg, 2011. **49**(7): p. 562-6.
52. Dempsey, J.A., et al., *Anatomic determinants of sleep-disordered breathing across the spectrum of clinical and nonclinical male subjects.* Chest, 2002. **122**(3): p. 840-51.
53. Izuka, E.N., M.F. Feres, and S.S. Pignatari, *Immediate impact of rapid maxillary expansion on upper airway dimensions and on the quality of life of mouth breathers.* Dental Press J Orthod, 2015. **20**(3): p. 43-9.
54. Hirshkowitz, M., *Monitoring techniques for evaluating suspected sleep-disordered breathing.* Sleep Medicine, 2005.
55. Janbakhshi, P. and M. Shamsollahi, *Sleep apnea detection from single-lead ECG using features based on ECG-derived respiration (EDR) signals.* IRBM, 2018. **39**(3): p. 206-218.
56. Solé-Casals, J., et al., *Detection of severe obstructive sleep apnea through voice analysis.* Applied Soft Computing, 2014. **23**: p. 346-354.
57. Mendonça, F., et al., *Devices for home detection of obstructive sleep apnea: A review.* Sleep medicine reviews, 2018. **41**: p. 149-160.
58. Pombo, N., N. Garcia, and K. Bousson, *Classification techniques on computerized systems to predict and/or to detect Apnea: A systematic review.* Computer methods and programs in biomedicine, 2017. **140**: p. 265-274.
59. Al-Mardini, M., et al., *Classifying obstructive sleep apnea using smartphones.* Journal of biomedical informatics, 2014. **52**: p. 251-259.
60. Sittitavornwong, S., et al., *Computational fluid dynamic analysis of the posterior airway space after maxillomandibular advancement for obstructive sleep apnea syndrome.* Journal of Oral and Maxillofacial Surgery, 2013. **71**(8): p. 1397-1405.
61. Yu, C.-C., et al., *Computational fluid dynamic study on obstructive sleep apnea syndrome treated with maxillomandibular advancement.* Journal of Craniofacial

Surgery, 2009. **20**(2): p. 426-430.

62. Sung, S.-J., et al., *Customized three-dimensional computational fluid dynamics simulation of the upper airway of obstructive sleep apnea.* The Angle Orthodontist, 2006. **76**(5): p. 791-799.

63. Yajima, Y., et al., *Computational fluid dynamics study of the pharyngeal airway space before and after mandibular setback surgery in patients with mandibular prognathism.* Int J Oral Maxillofac Surg, 2017. **46**(7): p. 839-844.

Figures

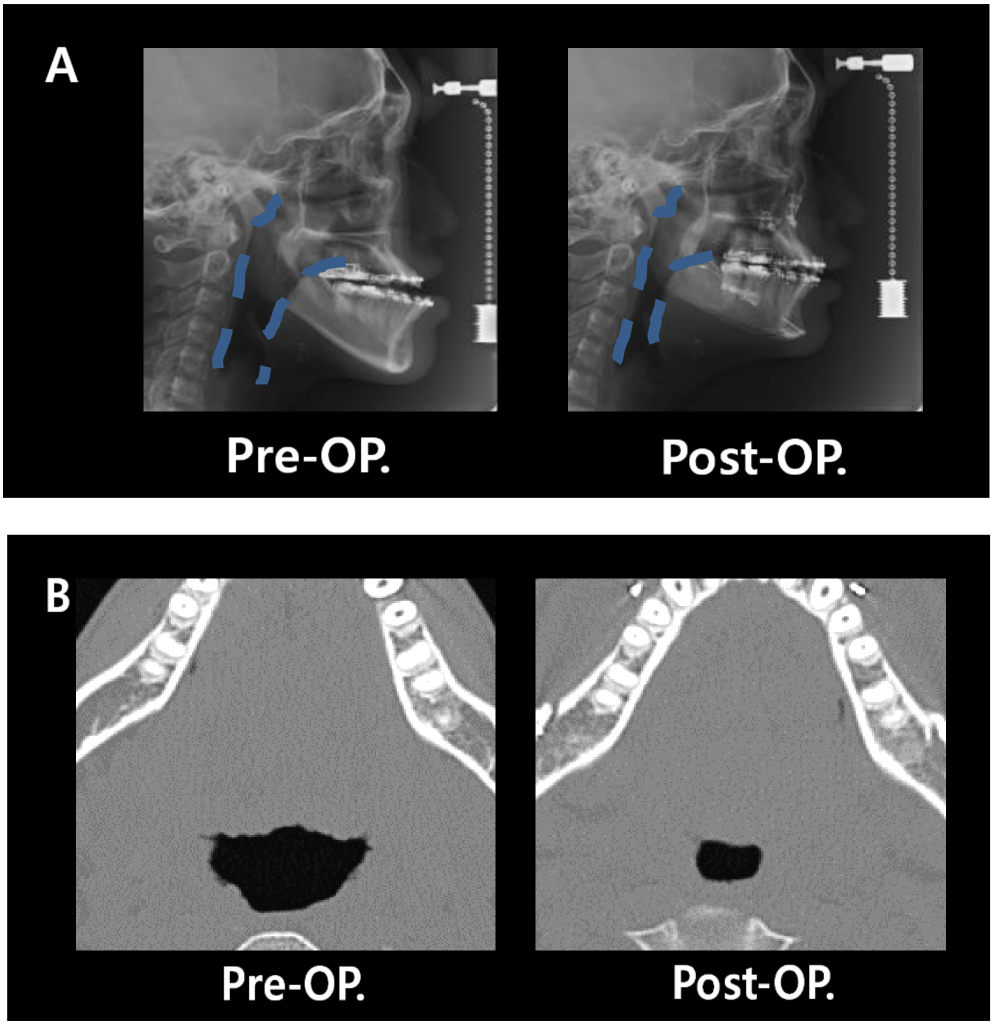

Figure 1

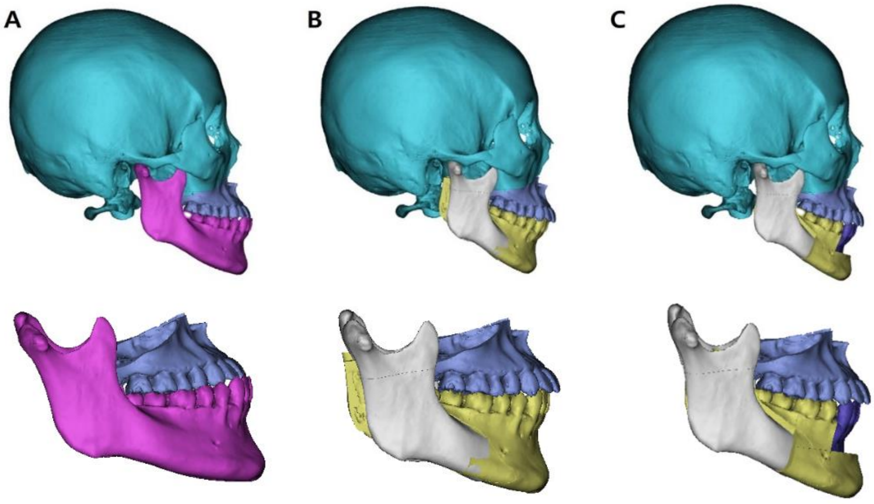

Figure 2

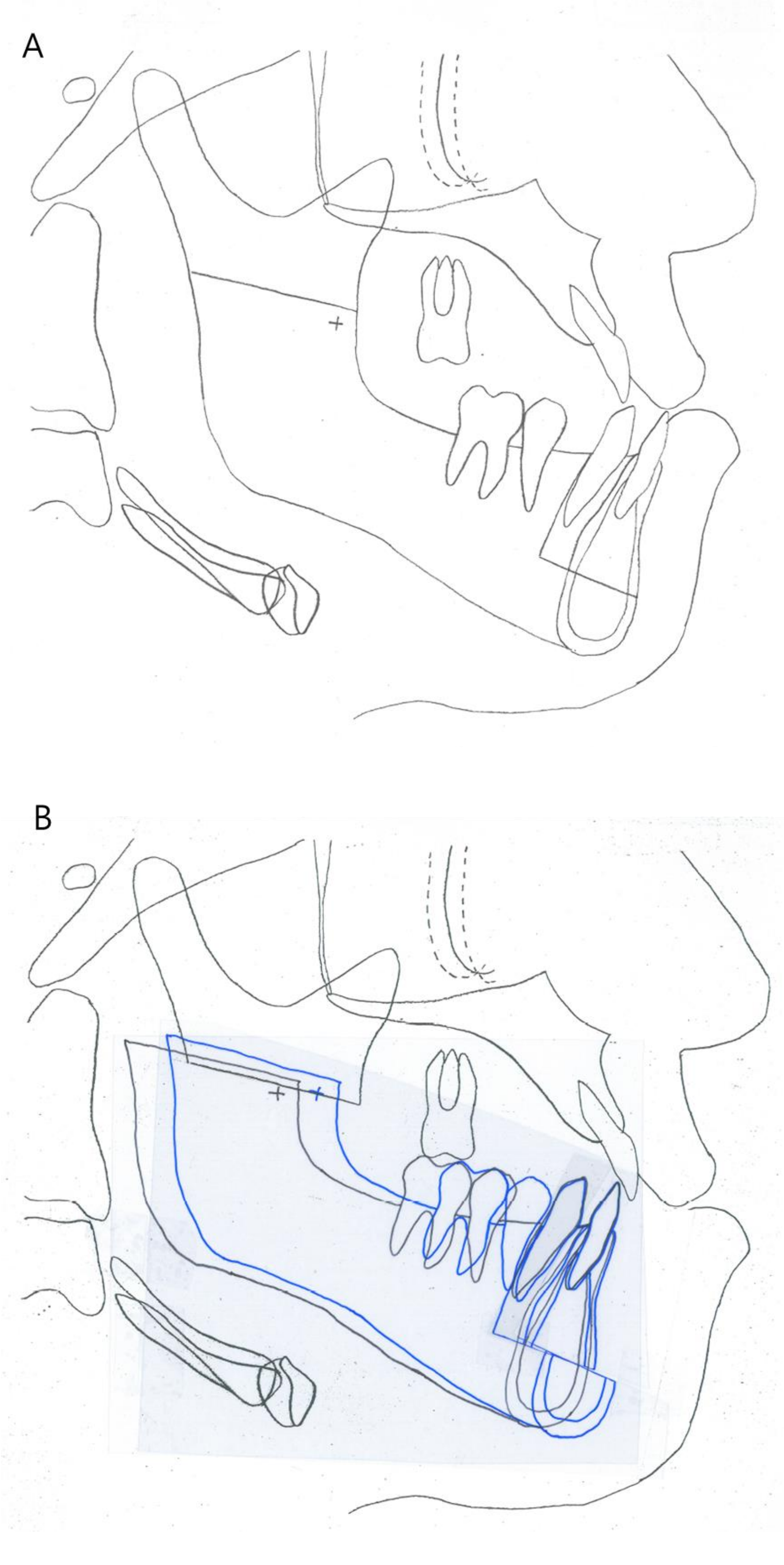

Figure 3

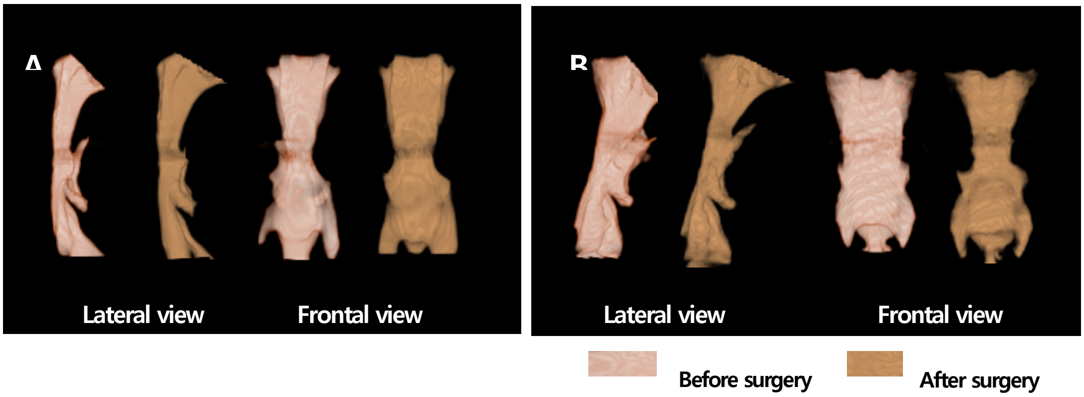
A
B
Lateral view
Frontal view
Lateral view
Frontal view
Before surgery
After surgery

Figure 4

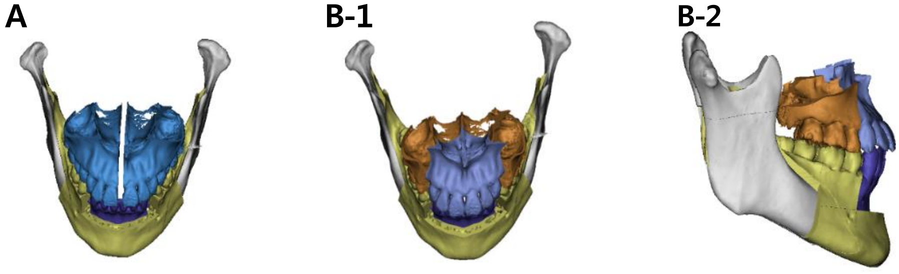

Figure 5

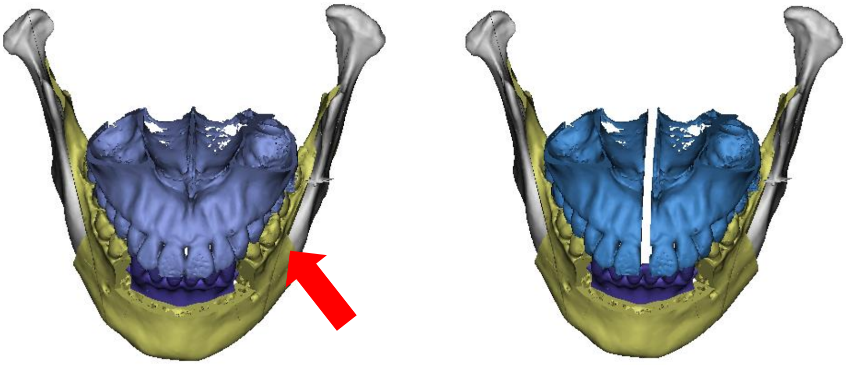

Figure 6

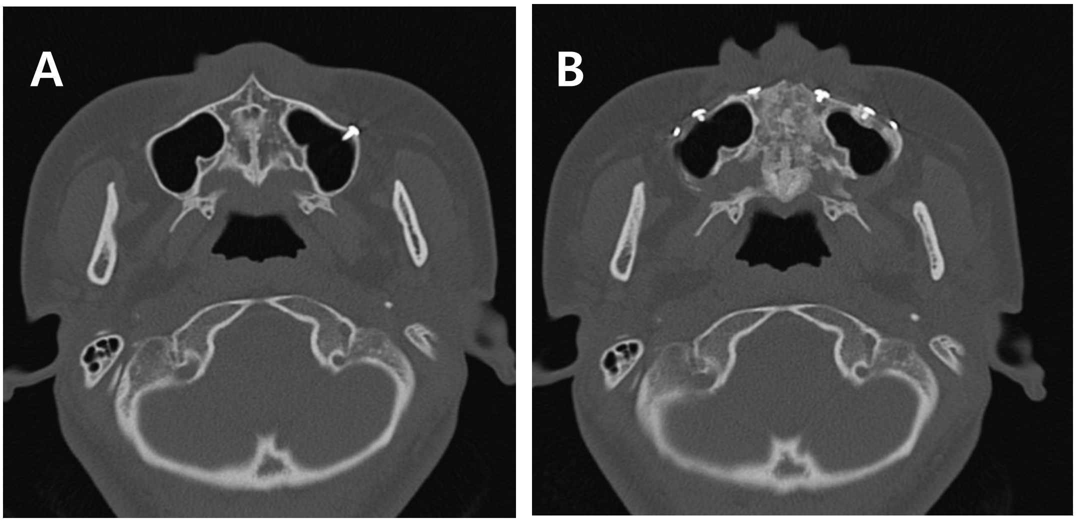

Figure 7

A: before surgery; B: 6 months after surgery.

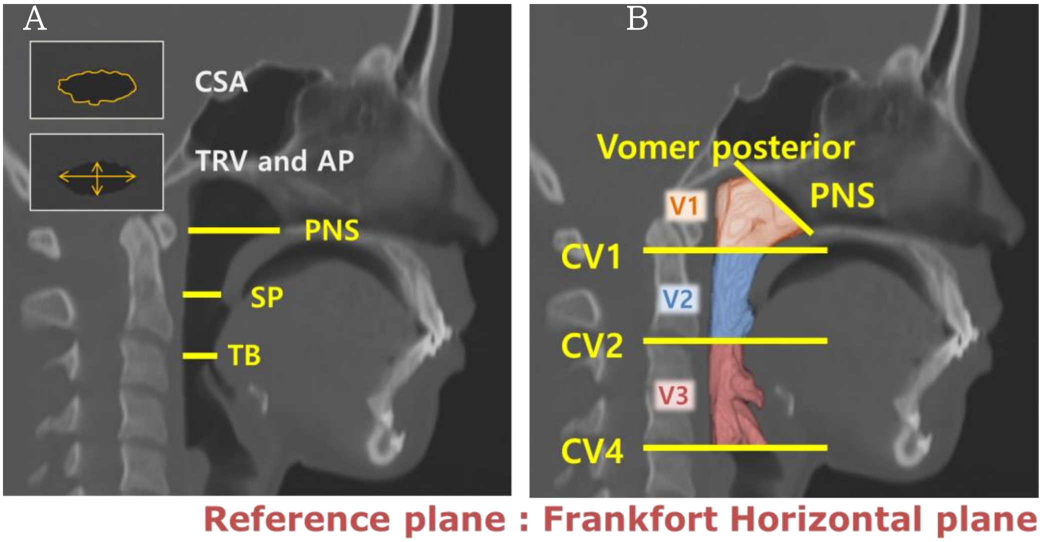
A
CSA
TRV and AP
PNS
SP
TB
B
Vomer posterior
PNS
V1
CV1
V2
CV2
V3
CV4
Reference plane : Frankfort Horizontal plane

Figure 8

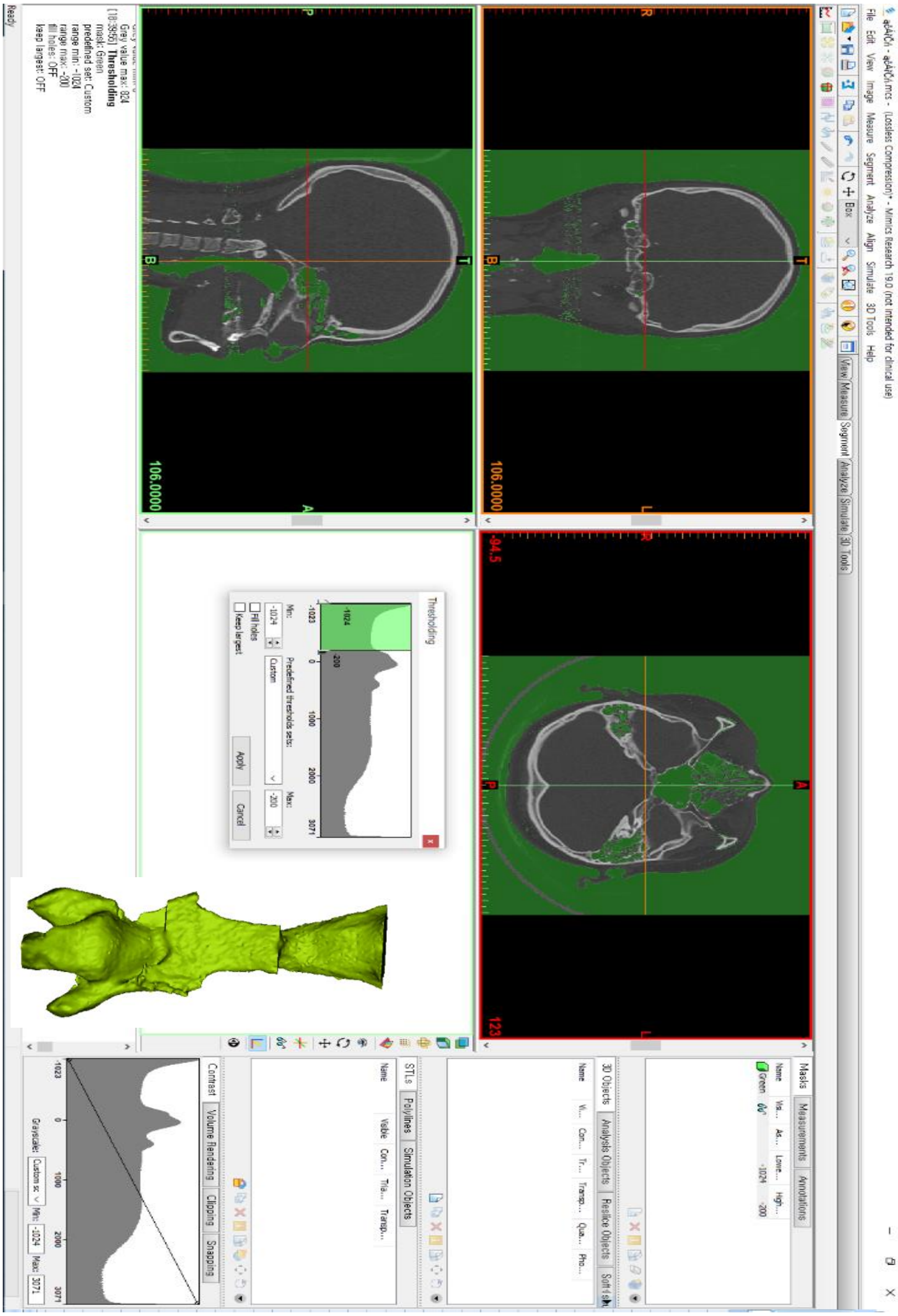

Figure 9

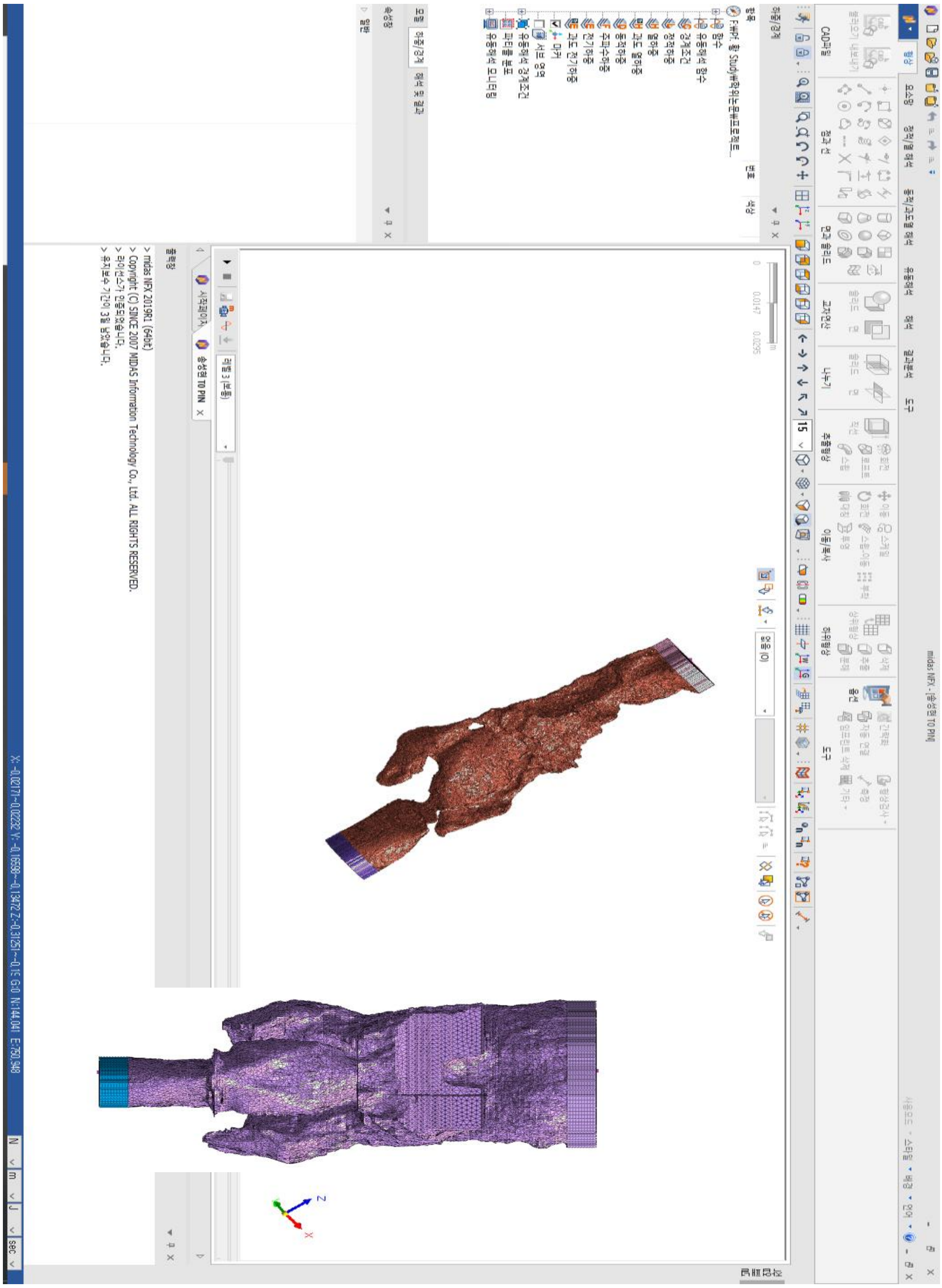

Figure 10

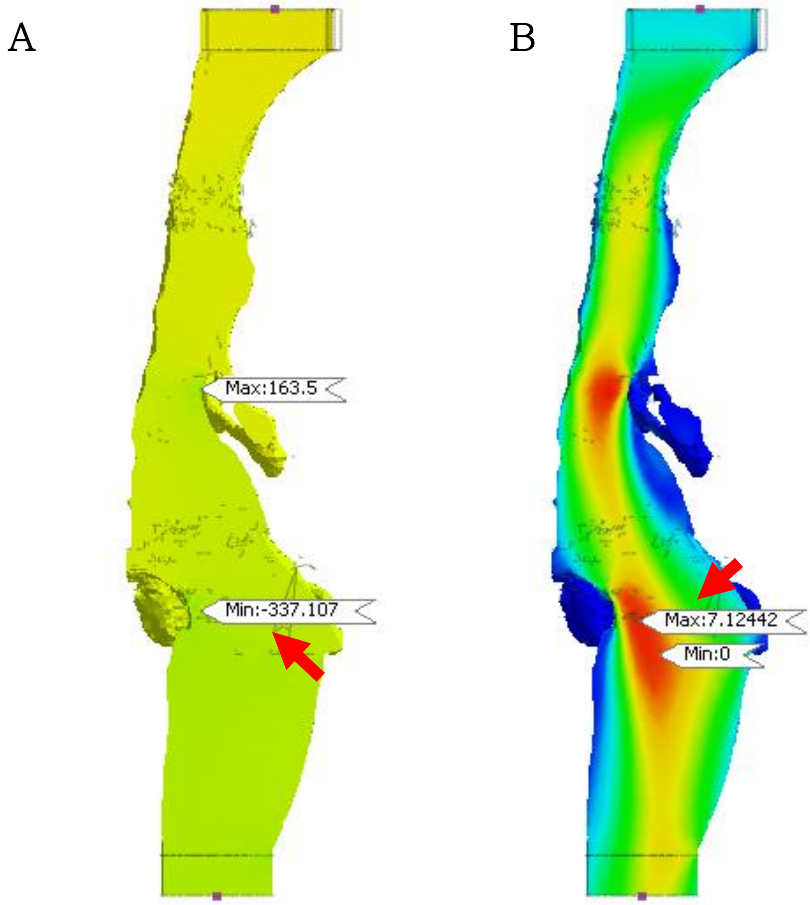

Figure 11

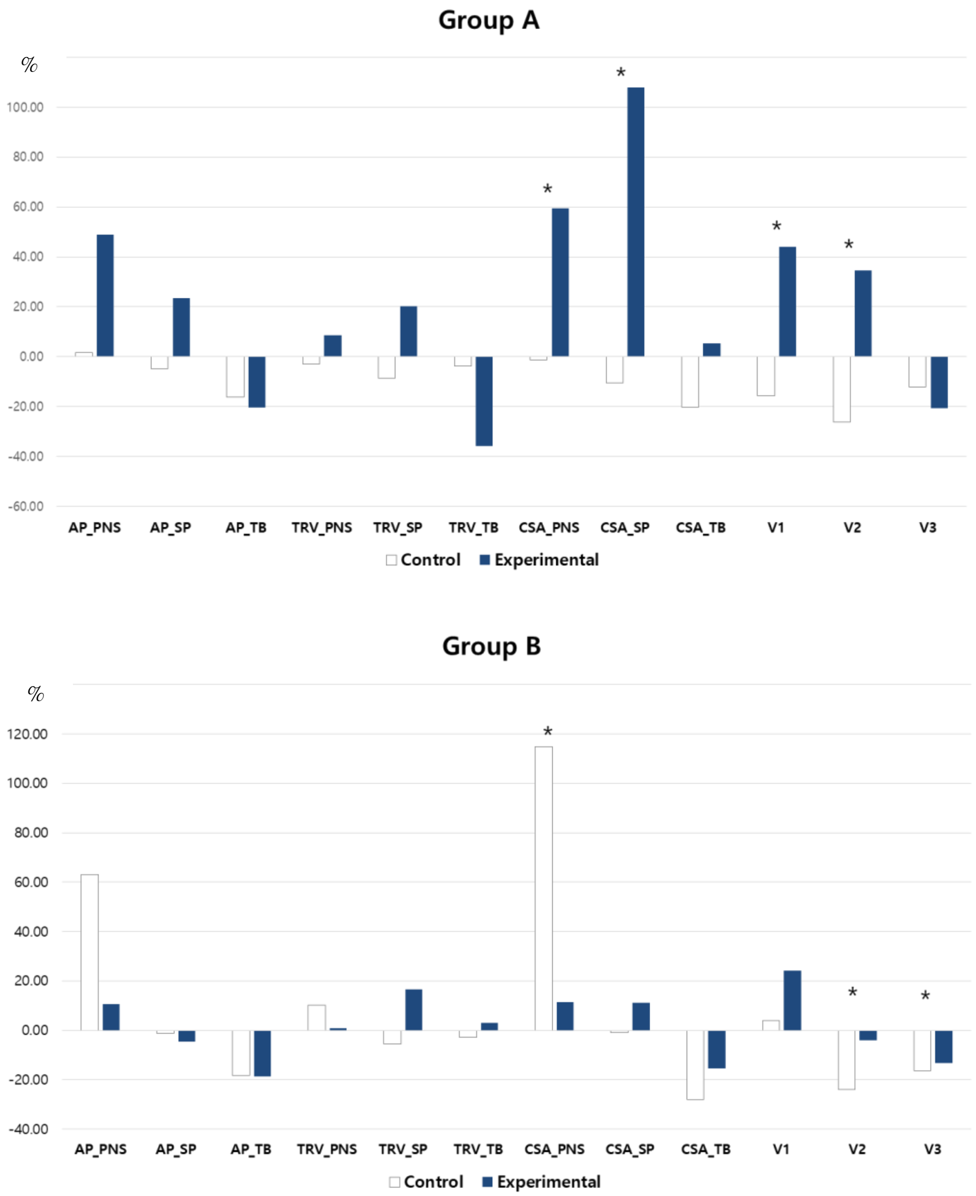

*** Statistically Significant (p<0.05)**
(+): Increased (-): Decreased

Figure 12

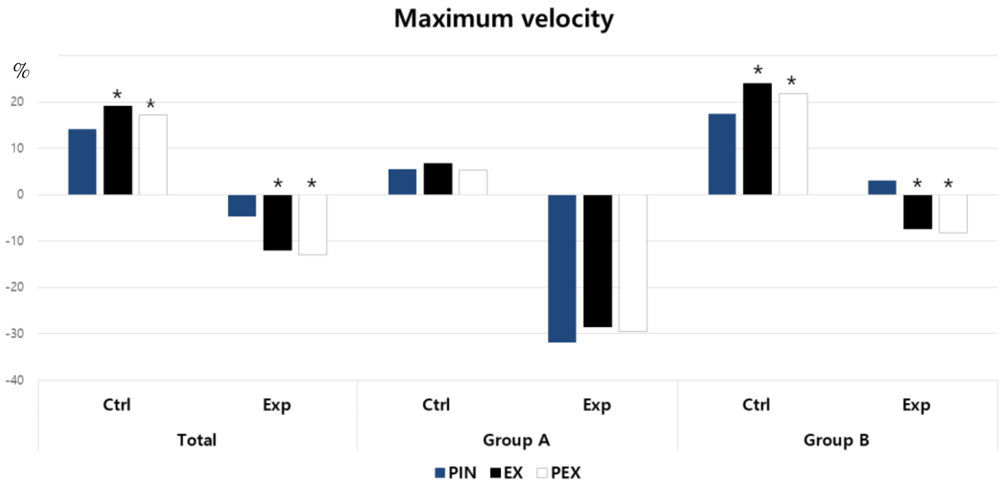

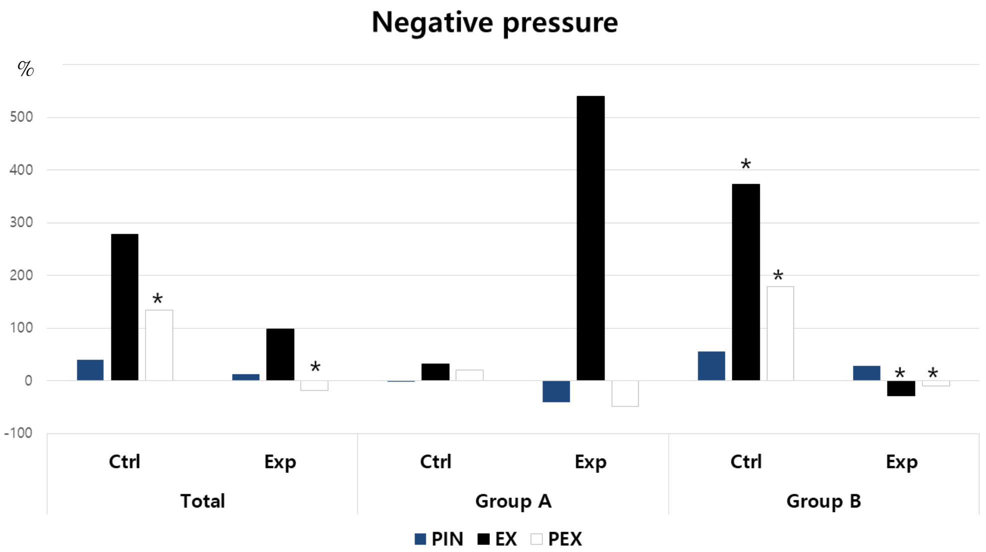

*** Statistically Significant ($p<0.05$)**

(+): Decreased negative pressure, (-): Increased negative pressure

Figure 13

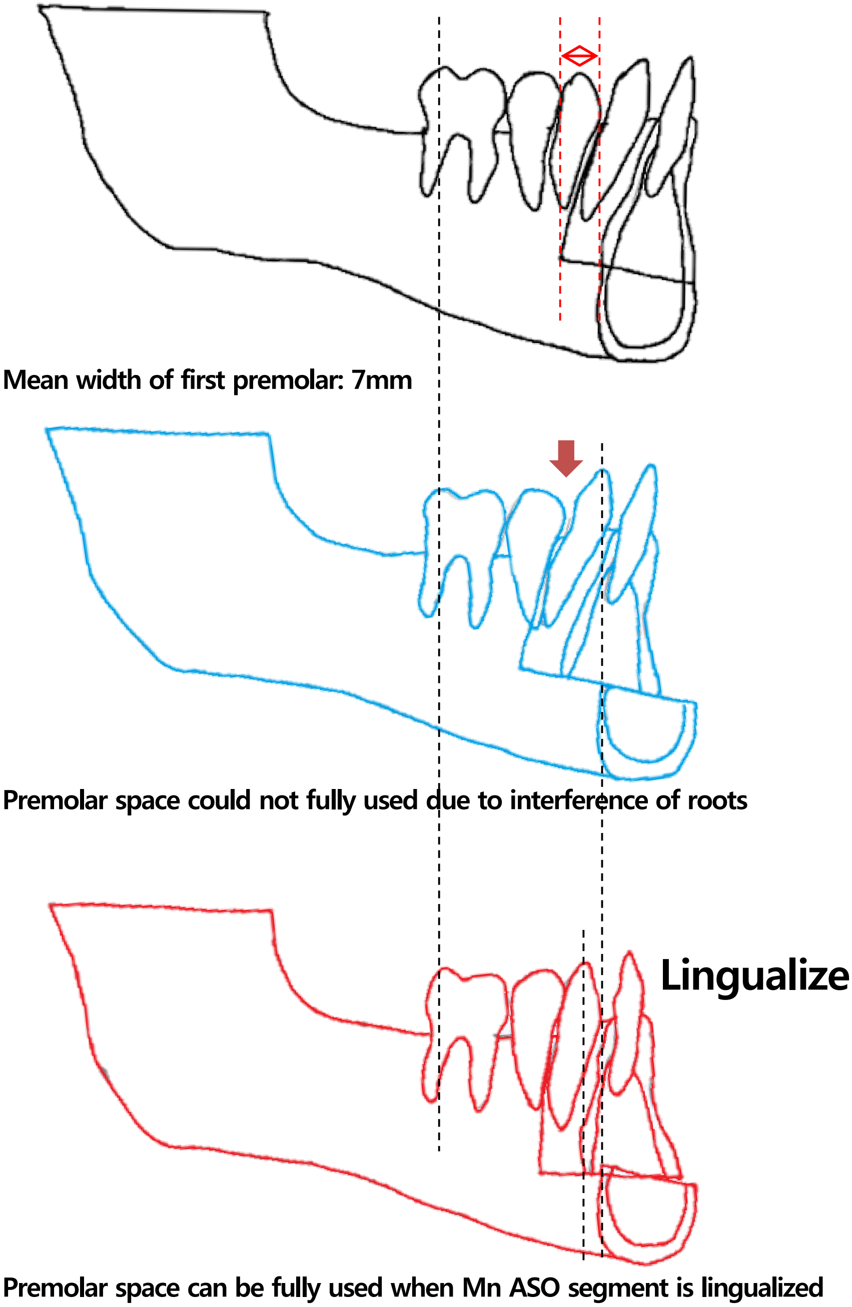
Mean width of first premolar: 7mm
Premolar space could not fully used due to interference of roots
Lingualize
Premolar space can be fully used when Mn ASO segment is lingualized

Figure 14

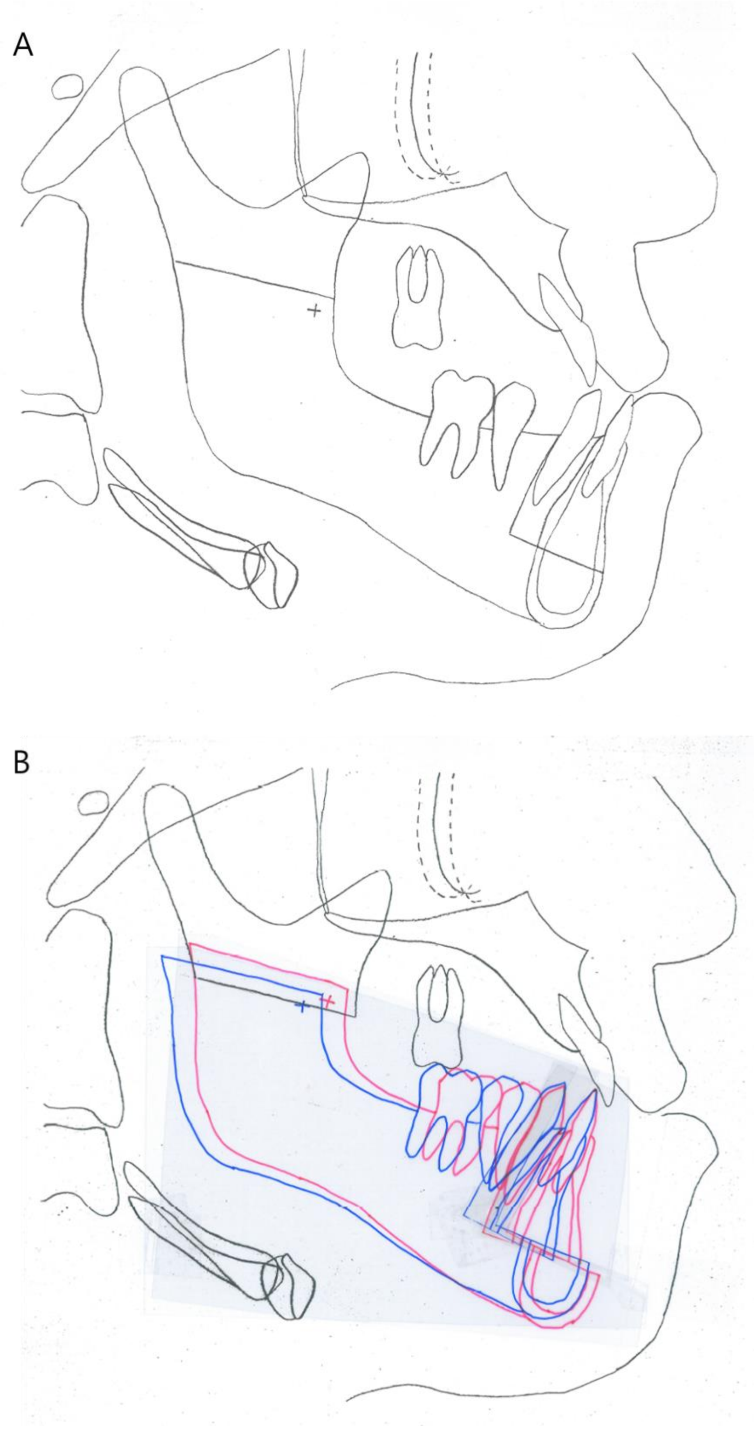

Figure 15

Figure Legends

Figure 1. Reduced pharyngeal airway space after mandibular setback movement.

Figure 2. Position of distal segment in virtual mandibular setback surgery with and without anterior segmental osteotomy.

A: skull and maxillomandibular complex before surgery; B: maxillomandibular complex after sagittal split ramus osteotomy without anterior segmental osteotomy; C: maxillomandibular complex after sagittal split ramus osteotomy with anterior segmental osteotomy. The posterior part of the distal segment after ASO moves it forward to close the extraction space of the 1st premolar. Central incisors are in identical positions after both surgical techniques.

Figure 3. Comparison of distal segment position after mandibular setback movement using sagittal split ramus osteotomy with anterior subapical osteotomy. A: before surgery, B: after surgery (ASO; blue line) and without ASO (black line). The posterior part of the distal segment moves forward after ASO to close the extraction space of the 1st premolar, whereas the central incisors are in identical positions after both surgical techniques.

Figure 4. Volume changes in pharyngeal airway space caused by two surgical methods for patients with mandibular prognathism.

A: sagittal split ramus osteotomy with anterior subapical osteotomy; B: sagittal split ramus osteotomy only. The amount of mandibular setback at the mandibular central incisor was identical in A and B.

Figure 5. Virtual maxillary expansion surgery and anterior segmental osteotomy.

A: maxillary transversal expansion with mandibular setback using sagittal split ramus osteotomy with anterior segmental osteotomy; B-1 and B-2: sagittal split ramus osteotomy with maxillary and mandibular anterior segmental osteotomy.

Figure 6. Virtual surgery of maxillary expansion to overcome posterior cross-bite.

Posterior cross-bite occurs when the mandibular moves backwards during SSRO combined with ASO.

Figure 7. Increased airway space after maxillary expansion.

Figure 8. Evaluation of postoperative changes in the pharyngeal airway.

A: distance and area; B: volume. The Frankfort horizontal plane is used as reference plane.

CSA: cross-sectional area; TR: transversal distance; AP: anterior–posterior distance; PNS: posterior nasal spine; SP: soft palate; TB: tongue base; and CV: cervical vertebrae.

Figure 9. Construction of individualized 3D airway model.

The 3D airway model was made with imported digital image files using the Mimics program (Materialise, Leuven, Belgium).

Figure 10. Mesh generation with airway model.

This model was extracted in stereolithography file format by Midas NFX CFD® (Midas IT, Seongnam, Korea) composed of tetrahedron and prism elements.

Figure 11. Measurement of maximum negative pressure (A) and maximum airflow velocity (B) using a commercial CFD package , Midas NFX CFD® (Midas IT, Seongnam, Korea).

Figure 12. Postoperative airway change (rate) analysis in subgroups A and B.

Group A: patients with mandibular setback < 10 mm; Group B: patients with mandibular setback ≥ 10 mm

Figure 13. Postoperative change in maximum air velocity and negative pressure in all patients in subgroups A and B.

PIN: peak of inspiration; EX: end of the expiration; PEX: peak of expiration.

Figure 14. Surgical maneuver for the overuse of premolar space by the lingualized segment

after anterior segmental osteotomy (ASO).

Figure 15. Lingualized segment after anterior segmental osteotomy (ASO) and decreased amount of mandibular setback. A: before surgery, B: after suftery

Tables

Classification according to the amount of mandibular setback	Experimental group (with ASO; n = 11)	Control group (without ASO; n = 33)
Group A (< 10 mm)	n = 3	n = 9
Group B (≥ 10 mm)	n = 8	n = 24

Table 1. Classification of patients

Both the experimental and control groups were divided into two subgroups (Groups A and B) according to the SB amount of the second molar (Group A: SB < 10 mm; Group B: SB ≥ 10 mm)

Table 2. Surgical movement of maxillary ASO and expansion and corresponded changes of nasopharynx

	#7_(mm)	Efficacy (mm)	AP_PNS (%)	TRV_PNS (%)	CSA_PNS (%)	V1 (%)
Maxillary ASO (n = 3)	-2.56±2.1 at crown -2.68±2.7 at root	7.28±0.58 at crown 1.53±4.73 at root	23.59±7.16	-2.2±14.94	28±43.81	33.67±38.27
Maxillary Expansion (n = 7)		6.56±4.1 at crown 5.25±2.43 at root	19.19±37.13	3.57±16.5	21.95±39.13	26.39±23.57
Orthodontic treatment (n = 1)		0.86 at crown -1.275 at root	26.98	13.97	33.45	38.92

#7: amount of maxillary #7 tooth movement (+ : posterior, - : anterior)

Eff: efficiency of ASO at #3 crown and root tip, efficacy of palatal expansion at #7 crown and palatal root tip

AP_PNS: anterior-posterior distance of airway in the level of the posterior nasal spine (PNS) parallel to the FH plane

TRV_PNS: transverse distance of airway in the level of the posterior nasal spine (PNS) parallel to the FH plane

CSA_PNS: cross-sectional area of airway in the level of the posterior nasal spine (PNS) parallel to the FH plane

V1: nasopharyngeal volume between PNS-Vp and CV1 plane

Table 3. Surgical movements (mm)

	A point (mm)	B point (mm)	Mandibular canine tip (mm)	Mandibular 2nd molar cusp* (mm)
Experimental Gr.	−0.35 ± 2.53	12.94 ± 5.93	12.84 ± 5.67	5.13 ± 6.33
Control Gr.	−1.07 ± 1.87	10.04 ± 3.01	-	10.52 ± 2.76
p-value	0.384	0.107	-	0.008

Described as mean ± standard deviation

* distobuccal cusp

Table 4. Efficiency of anterior segmental osteotomy on the reduction of mandibular setback movement

	Reduction in the amount of mandibular setback movement by ASO (mm)	Range (mm)
At canine cusp	7.01 ± 2.38	2.12–9.90
At canine root tip	6.46 ± 2.26	1.02–9.42

Table 5. Postoperative airway changes in all patients

	Experimental Gr. (with ASO)			Control Gr. (without ASO)		
	preop.	postop.	*p*-value	preop.	postop.	*p*-value
AP_PNS (mm)	17.35 ± 4.28	20.12 ± 3.05	0.041*	20.82 ± 6.06	22.12 ± 4.26	0.228
AP_SP (mm)	8.55 ± 2.9	8.29 ± 1.9	0.79	9.77 ± 2.73	8.58 ± 1.75	0.014*
AP_TB (mm)	12.55 ± 3.97	10.35 ± 4.01	0.021*	14 ± 4.98	11.13 ± 3.02	<0.001*
TRV_PNS (mm)	25.52 ± 3.2	26.07 ± 3.9	0.534	27.34 ± 4.35	27.65 ± 2.99	0.915
TRV_SP (mm)	16.61 ± 4.84	18.87 ± 4.85	0.091	21.92 ± 5.66	19.6 ± 5.7	0.002*
TRV_TB (mm)	20.76 ± 4.89	19.48 ± 8.51	0.657	28.04 ± 6.8	26.11 ± 5.22	0.012*
CSA_PNS (mm^2)	390.79 ± 70.39	473.71 ± 118.13	0.075	464.13 ± 145.05	483.96 ± 111.06	0.636
CSA_SP (mm^2)	121.91 ± 51.75	152.02 ± 69.46	0.248	195.69 ± 123.48	146.5 ± 68.83	0.002*
CSA_TB (mm^2)	195.45 ± 84.55	177.76 ± 88.65	0.374	297.01 ± 107.44	218.17 ± 89.96	<0.001*

V1 (cc)	6.69 ± 1.84	8.41 ± 1.63	0.006*	8.22 ± 2.21	7.77 ± 2.38	0.081
V2 (cc)	4.14 ± 1.48	4.2 ± 1.32	0.929	6.87 ± 3.06	5.06 ± 2.05	<0.001*
V3 (cc)	9.04 ± 3.49	8.12 ± 4.05	0.091	9.56 ± 2.12	8.28 ± 2.63	0.002*

AP_PNS: Anterior-posterior distance (mm) of airway the level of the posterior nasal spine (PNS) parallel to the FH plane

AP_SP: Anterior-posterior distance (mm) of airway the level of the soft palate (SP) parallel to the FH plane

AP_TB: Anterior-posterior distance (mm) of airway the level of the tongue base (TB) parallel to the FH plane

TRV_PNS: Transverse distance (mm) of airway the level of the posterior nasal spine (PNS) parallel to the FH plane

TRV_SP: Transverse distance (mm) of airway the level of the soft palate (SP) parallel to the FH plane

TRV_TB: Transverse distance (mm) of airway the level of the tongue base (TB) parallel to the FH plane

CSA_PNS: Cross-sectional area of airway (mm2) the level of the posterior nasal spine (PNS) parallel to the FH plane

CSA_SP: Cross-sectional area of airway the level of the soft palate (SP) parallel to the FH plane

CSA_TB: Cross-sectional area of airway the level of the tongue base (TB) parallel to the FH plane

V1: Nasopharyngeal volume between PNS-Vp and CV1 plane

V2: Oropharyngeal volume between CV1 and CV2 planes

V3: Hypopharyngeal volume between the CV2 and CV4 planes

Table 6. Postoperative airway changes in subgroups (%)

	Group A (<10 mm)			Group B (≥10 mm)		
	Control Gr.	Exp. Gr.	*p*-value	Control Gr.	Exp. Gr.	*p*-value
AP_PNS (%)	1.59 ± 26.82	49.03 ± 39.61	0.08	63.02 ± 149.62	10.62 ± 17.3	0.66
AP_SP (%)	−4.89 ± 17.56	23.47 ± 44.88	0.17	−1.11 ± 51.49	−4.6 ± 19.53	0.57
AP_TB (%)	−16.06 ± 21.91	−20.21 ± 69.54	0.52	−18.4 ± 26.64	−18.74 ± 11.76	0.83
TRV_PNS (%)	−2.96 ± 15.18	8.53 ± 18.61	0.31	10.24 ± 31.9	0.84 ± 14.45	0.83
TRV_SP (%)	−8.58 ± 14.11	20.14 ± 35.4	0.31	−5.48 ± 17.81	16.54 ± 24.36	0.01*
TRV_TB (%)	−3.77 ± 17.77	−35.85 ± 60.53	0.41	−2.95 ± 34.62	2.88 ± 13.98	0.19
CSA_PNS (%)	−1.37 ± 25.57	59.63 ± 36.42	0.03*	114.85 ± 341.41	11.53 ± 28	0.66
CSA_SP (%)	−10.49 ± 27.28	108.05 ± 35.8	0.01*	−0.84 ± 75.7	11.1 ± 51.81	0.18
CSA_TB (%)	−20.15 ± 25.13	5.44 ± 91.76	0.41	−28.18 ± 28.15	−15.54 ± 29.93	0.18

V1 (%)	−15.63 ± 29.59	44.02 ± 37.2	0.05*	4.05 ± 27.52	24.08 ± 20.12	0.03*
V2 (%)	−26.14 ± 22.45	34.65 ± 13.74	0.01*	−23.89 ± 19.49	−4.16 ± 25.24	0.05*
V3 (%)	−12.02 ± 17.21	−20.66 ± 48.53	0.64	−16.4 ± 21.86	−13.23 ± 18.97	0.38

* Mann–Whitney U test

AP_PNS: Anterior-posterior distance (mm) of airway the level of the posterior nasal spine (PNS) parallel to the FH plane

AP_SP: Anterior-posterior distance (mm) of airway the level of the soft palate (SP) parallel to the FH plane

AP_TB: Anterior-posterior distance (mm) of airway the level of the tongue base (TB) parallel to the FH plane

TRV_PNS: Transverse distance (mm) of airway the level of the posterior nasal spine (PNS) parallel to the FH plane

TRV_SP: Transverse distance (mm) of airway the level of the soft palate (SP) parallel to the FH plane

TRV_TB: Transverse distance (mm) of airway the level of the tongue base (TB) parallel to the FH plane

CSA_PNS: Cross-sectional area of airway (mm2) the level of the posterior nasal spine (PNS) parallel to the FH plane

CSA_SP: Cross-sectional area of airway the level of the soft palate (SP) parallel to the FH plane

CSA_TB: Cross-sectional area of airway the level of the tongue base (TB) parallel to the FH plane

V1: Nasopharyngeal volume between PNS-Vp and CV1 plane

V2: Oropharyngeal volume between CV1 and CV2 planes

V3: Hypopharyngeal volume between the CV2 and CV4 planes

Table 7. Postoperative change in maximum air velocity and peak negative pressure (%)

		rPIN vMax	rPIN neg Pr	rEX vMax	rEX neg Pr	rPEX vMax	rPEX neg Pr
Total patient	Control Gr.	14.07 ±32.34	40.32 ±103.99	19.11 ±37.11	277.55 ± 1097.75	17.17 ± 36.31	134.44 ±318.93
	Experimental Gr.	−4.68 ±28.79	13.25 ±82.15	−12.04 ± 30.78	98.19 ±391.38	−12.99 ± 34.4	−17.54 ±61.63
	p-value	0.063	0.378	0.018*	0.095	0.014*	0.012*
Group A (<10 mm)	Control Gr.	5.42 ± 26.11	−0.93 ±52.3	6.69 ±26.49	32.51 ±107.97	5.28 ± 23.91	21.33 ±68.19
	Experimental Gr.	−31.93 ± 9.17	−40.39 ±5.39	−28.55 ± 18.72	539.73 ±840.49	−29.57 ± 10.6	−47.86 ±15.6
	p-value	0.059	0.346	0.059	0.48	0.059	0.239
Group B (≥10 mm)	Control Gr.	17.45 ±34.4	56.46 ±115.21	23.96 ±39.97	373.43 ± 1288.27	21.83 ± 39.61	178.7 ±366.54
	Experimental	3.11	28.57	−7.32 ±	−27.96	−8.25 ±	−8.88

Gr.	±27.79	±88.09	32.99	±54.27	37.96	±68.04
p-value	0.082	0.267	0.018*	0.013*	0.016*	0.013*

PIN: peak of inspiration, EX: end of the expiration, PEX: peak of expiration

vMax: maximum velocity; (+): increase, (-): decrease

neg Pr: negative pressure; (+): increase, (-): decrease

*Mann–Whitney U test

- 국문초록 -

하악 후방이동 악교정수술에서 부가적인 악골의 분절골 절단술이 상기도 공간 변화에 미치는 영향에 대한 연구

조 예 원
서울대학교 치의학대학원
치의과학과 구강악안면외과학 전공
(지도교수 김 성 민)

1. 목 적

하악골의 후방이동을 동반한 악교정수술을 시행받는 환자에서 술전 기도공간 체적이 적거나 예상되는 하악 후퇴량이 큰 경우, 술후 기도 공간이 감소하고 결과적으로 수면 무호흡의 위험에 노출될 수 있다. 하악 후퇴량을 줄이기 위해 상악골의 전방 이동을 동반하는 방법을 생각할 수 있으나 코가 작고 낮으며 구순부가 돌출된 동북 아시아인의 안모에서 상악골의 전방 이동량에 제한이 있을 수 밖에 없다. 심미적인 안모 형태를 유지함과 동시에 하악골의 후퇴량을 줄이기 위해 하악 전방부 근첨하 골절단술을 동반한 하악지 시상분할 골절단술이 보고되었지만, 아직 이에 대한 기도공간 감소 효과가 보고된 바가

없다. 본 연구에서는 하악골의 후방이동을 동반한 악교정수술을 시행받는 환자에서 심미적인 안모 형태를 유지함과 동시에 하악골의 후퇴량을 줄여 하악의 후퇴에 따른 기도공간의 감소 및 수면무호흡 발생의 위험을 줄이기 위해 부가적으로 시행된 악골의 분절골절단술이 상기도 공간증감에 미치는 효과에 대해서 분석하였으며 호흡에 따른 기도 저항에 대한 가상분석을 통해 추가적으로 부가적인 악골 분절골절단술이 미치는 영향에 대해 평가하고자 하였다.

2. 방 법

골격성 제 3급 부정교합으로 하악지 시상분할 골절단술 과 LeFort 씨 제 1형 골 절단술 시행받은 44명의 환자를 대상으로 연구를 수행하였다. 하악 전방부 근첨하 골절단술을 함께 시행받은 11명의 환자를 실험군으로 설정하였고 이에 따른 상악의 폭경 부조화는 상악 폭경확장수술(7명), 상악 전방분절골절단술(3명) 또는 교정적 치료(1명)로 개선하였고, 이로 인한 기도 공간의 변화가 포함된 상기도 공간을 분석하였다. 실험군 환자들이 하악 전방부 근첨하 골절단술을 동반하지 않았을 경우에 해당되는 가상의 수술량을 기준으로 하악 전방부 근첨하 골절단술 없이 하악지 시상분할 골절단술만 시행받은 33명의 환자를 대조군으로 설정하였다. 환자들은 수술량에 따라 두개 집단으로 나뉘었으며 (A군: 하악 후퇴량 10mm 미만, B군: 하악 후퇴량 10mm 이상), 각 환자에서 술전 및 술후 3-6개월 시기의 컴퓨터단층영상

이미지에서 기도공간의 단면적, 종단길이, 횡단길이, 부피를 측정하였고, 이들 환자에서 공기흐름을 유체역학적으로 가상 분석하여 기도 저항에 대해서 평가하였다.

3. 결 과

실험 군에서 상악 전방분절골절단술 시행한 환자는 약 2.5mm 정도 상악이 전진된 것으로 평가되었고 비인두부 단면적 약 28 %, 비인두 부피는 33.67 % 증가하였다. 상악 폭경확장술 시행한 환자에서 평균 확장량은 6.56mm였다. 비인두부 단면적은 21.95 % 증가하였고 비인두 부피는 26.39 % 증가하였다. 하악 전방부 근첨하 골절단술은 치관부에서 7.01 ± 2.38mm, 치근부에서 6.46 ± 2.26mm의 하악 후방이동 감소 효과가 보였다. A군에서 구개후방부의 기도 단면적, 비인두강 및 구인두강의 부피는 대조군에서 현저한 감소를 보였지만 실험군에서는 증가하였다 ($p < 0.05$). B군에서, 구개후방부의 횡단길이, 구인두강의 부피는 대조군 에서 감소하였으며 실험군 에서 증가하였다 ($p < 0.05$). 비인두강 부피는 대조군 및 실험군 에서 모두 증가하였으나 실험군 에서 더 많이 증가하였다 ($p < 0.05$). 기도공간의 공기 흐름 분석 결과 B군에서 최대 공기 유속은 수술 전,후 통계적으로 유의미하게 실험군 에서 감소하였고 대조군 에서 증가하였다.

4. 결 론

하악의 후퇴를 동반하는 악교정 수술 시행 환자에서 전방부 근첨하 골절단술을 동반하는 경우 하악 후퇴량을 줄일 수 있었고, 기도공간의 단면적 및 부피의 수술 전후 감소하는 것을 방지할 수 있었다. 또한 기도공간 내 공기흐름을 악화시키는 효과를 줄일 수 있었다. 수면무호흡증의 발병 감소에 대한 효과는 추가적인 수면다원검사가 동반된 추가 연구가 필요하다.

주요어 : 과두 변위, 시상 분할 하악지 골절단술, 관절와 깊이
학번 : 2018-29027

감사의 글

무엇보다도, 가장 먼저, 존경하는 황순정 지도교수님께 감사 인사를 드립니다. 교수님께서 열성과 정성으로 지도해주시지 않았더라면 저는 결코 박사학위를 받지 못했을 것입니다. 퇴임하시어 외부에 계신 와중에도 바쁜 시간을 쪼개어 연구를 함께 고민해주시고 더 나은 논문이 되도록 지도해 주셨습니다. 포기하고 싶었던 매 순간, 교수님의 관심과 애정, 책임감 있는 지도에 힘입어 학위논문을 잘 마무리할 수 있었습니다. 그동안 보여드린 부족한 모습을 반성하며 앞으로 남은 시간 동안 교수님의 은혜에 보답할 수 있는 길을 걷겠습니다.

다음으로, 제 부족한 논문을 박사 논문답게 발전시키는데 큰 도움을 주신 서병무 교수님, 김성민 교수님, 최진영 교수님, 김태우 교수님께 감사 드립니다. 미숙한 논문이나마 따끔한 충고와 함께 더 나은 방향을 고민 해 주셔서 감사드립니다.

또한 논문의 질적 향상을 위해 도움 주신 여러 분들께 감사드립니다. 분석을 위한 프로그램 사용법을 교육해 주신 양훈주교수님께 감사드리며 유체역학 분석 프로그램을 제공해주신 마이다스아이티 사와 문외한이었던 유체역학 분석방법을 함께 고민해 주신 일산병원 구강악안면외과 김문기교수님께 크나큰 감사 인사 드립니다.

끝으로 늘 곁에서 함께해 준 배우자와 가족들에게 감사와 사랑을 드리며 작은 결실의 기쁨을 함께 하고자 합니다.

2020 년 1 월 21 일

조 예 원 드림